Acta Pharmaceutica Sinica B 2023;13(10):4202–4216

Chinese Pharmaceutical Association
Institute of Materia Medica, Chinese Academy of Medical Sciences

Acta Pharmaceutica Sinica B

www.elsevier.com/locate/apsb
www.sciencedirect.com

ORIGINAL ARTICLE

Gut microbiota controls the development of chronic pancreatitis: A critical role of short-chain fatty acids-producing Gram-positive bacteria

Li-Long Pan[a,†], Zheng-Nan Ren[b,c,†], Jun Yang[d,†], Bin-Bin Li[b,c,†], Yi-Wen Huang[b,c], Dong-Xiao Song[b,c], Xuan Li[b,c], Jia-Jia Xu[e], Madhav Bhatia[f], Duo-Wu Zou[g], Chun-Hua Zhou[g], Jia Sun[b,c,*]

[a]*Wuxi Medical School, Jiangnan University, Wuxi 214122, China*
[b]*School of Food Science and Technology, Jiangnan University, Wuxi 214122, China*
[c]*State Key Laboratory of Food Science and Resources, Jiangnan University, Wuxi 214122, China*
[d]*Department of General Surgery, Affiliated Hospital of Jiangnan University, Wuxi 214122, China*
[e]*Department of General Medicine, Beicai Community Health Service Center of Pudong New District, Shanghai 214001, China*
[f]*Department of Pathology, University of Otago, Christchurch 8140, New Zealand*
[g]*Department of Gastroenterology, Ruijin Hospital Affiliated to Shanghai Jiao Tong University School of Medicine, Shanghai 200025, China*

Received 28 February 2023; received in revised form 21 May 2023; accepted 13 June 2023

KEY WORDS

Chronic pancreatitis;
Antibiotic exposure;
Gut microbiota;
Short-chain fatty acids-producing bacteria;
Pancreatic fibrogenesis;
Macrophage responses;
Toll-like receptor 4;

Abstract Chronic pancreatitis (CP) is a progressive and irreversible fibroinflammatory disorder, accompanied by pancreatic exocrine insufficiency and dysregulated gut microbiota. Recently, accumulating evidence has supported a correlation between gut dysbiosis and CP development. However, whether gut microbiota dysbiosis contributes to CP pathogenesis remains unclear. Herein, an experimental CP was induced by repeated high-dose caerulein injections. The broad-spectrum antibiotics (ABX) and ABX targeting Gram-positive (G^+) or Gram-negative bacteria (G^-) were applied to explore the specific roles of these bacteria. Gut dysbiosis was observed in both mice and in CP patients, which was accompanied by a sharply reduced abundance for short-chain fatty acids (SCFAs)-producers, especially G^+ bacteria. Broad-spectrum ABX exacerbated the severity of CP, as evidenced by aggravated

*Corresponding author.
E-mail address: jiasun@jiangnan.edu.cn (Jia Sun).
[†]These authors made equal contributions to this work.
Peer review under the responsibility of Chinese Pharmaceutical Association and Institute of Materia Medica, Chinese Academy of Medical Sciences.

https://doi.org/10.1016/j.apsb.2023.08.002

Roseburia intestinalis

pancreatic fibrosis and gut dysbiosis, especially the depletion of SCFAs-producing G^+ bacteria. Additionally, depletion of SCFAs-producing G^+ bacteria rather than G^- bacteria intensified CP progression independent of TLR4, which was attenuated by supplementation with exogenous SCFAs. Finally, SCFAs modulated pancreatic fibrosis through inhibition of macrophage infiltration and M2 phenotype switching. The study supports a critical role for SCFAs-producing G^+ bacteria in CP. Therefore, modulation of dietary-derived SCFAs or G^+ SCFAs-producing bacteria may be considered a novel interventive approach for the management of CP.

1. Introduction

Chronic pancreatitis (CP) is a progressive inflammatory and fibrotic disease of the pancreas with no satisfactory cure[1]. CP is characterized by persistent inflammation and progressive fibrosis, leading to irreversible morphological changes of the gland, most notably parenchymal atrophy, along with gradual impairment of exocrine and endocrine functions[2]. To date, the incidence and prevalence of CP have been rising and no effective therapy is available to limit or reverse the inflammatory damage or pancreatic fibrosis associated with CP[2]. CP reduces patients' quality of life and is also a significant risk factor for developing pancreatic cancer[3]. Further understanding of the disease pathogenesis and identification of novel player(s) that contribute to it are required for the development of novel therapeutic strategies for CP.

Accumulating evidence has supported the association of gut dysbiosis with the development of CP. A large number of CP patients have intestinal bacterial overgrowth[4], which is closely associated with exocrine insufficiency[5]. Moreover, small intestinal bacterial overgrowth complicates CP and interferes with the therapy, which is supportive for the involvement of gut dysbiosis in CP[4,6,7]. An altered intestinal microbiota has been demonstrated in CP patients and experimental CP models[8,9]. At the *genus* level, the abundances of *Faecalibacterium* and *Subdoligranulum* are reduced, which have been demonstrated to have anti-inflammatory and barrier-protective effects[10,11]. In contrast, the pro-inflammatory *Escherichia-Shigella* are the dominant genera in the fecal microbiomes of CP patients[12]. Alterations in the gut microbiota composition were also observed in experimental CP mice, as evidenced by decreased abundances of *Lachnospiraceae_NK4A136*, *Ruminiclostridium* and *Roseburia* and increased abundance of *Bacteroides*[8]. Despite a rather established close association, few studies have looked into specific roles of different gut microbes in the pathogenesis of CP.

Pancreatic fibrosis is a major histological feature of CP, caused by uncontrolled activation and proliferation of pancreatic stellate cells (PSCs)[13,14] and dysregulated overproduction of extracellular matrix (ECM) proteins. Under steady-state, PSCs maintain the normal architecture of the pancreas by regulating the synthesis and degradation of ECM proteins[14]. Macrophages, particularly the alternatively activated or M2 macrophages, are thought to play an important role in regulating PSCs-mediated fibrogenesis. During CP pathogenesis, M2 macrophages secrete massive transforming growth factor-β and platelet-derived growth factor, resulting in aberrant activation of PSCs and massive synthesis of ECMs, eventually causing pancreatic fibrosis[15]. Thus, inhibition of M2-fibrogenesis represents a promising therapeutic approach for CP.

In the current study, we applied broad-spectrum antibiotics (ABX) and ABX targeting Gram-positive (G^+) or Gram-negative (G^-) bacteria to explore the specific roles of gut bacteria in CP. Our data reveal a vital role of short-chain fatty acids (SCFAs)-producing G^+ bacteria in the modulation of CP and the intervention strategy targeting commensal bacteria for the management of CP.

2. Materials and methods

2.1. Reagents

Caerulein was purchased from Ji Tai Peptide (Yancheng, China). Pentobarbital sodium, acetate, butyrate, propionate and fluorescein isothiocyanate (FITC)-dextran 4000 were purchased from Sigma−Aldrich (Shanghai, China). Vancomycin, neomycin, ampicillin and metronidazole were purchased from Sangon Biotech Co., Ltd. (Shanghai, China). RIPA Lysis Buffer was purchased from Beyotime (Shanghai, China). For immunofluorescence assay, the primary antibody for α-smooth muscle actin (α-SMA, 48938S) was purchased from Cell Signaling Technology (Danvers, MN, USA). Rabbit anti-mouse IgG (H + L) cross-adsorbed secondary antibody (A11059) was purchased from Thermo Fisher Scientific (Waltham, MA, USA). TRIzol reagent was purchased from Life Technologies (Waltham, MA, USA). 4′,6-Diamidino-2-phenylindole (DAPI) was purchased from Solarbio (Beijing, China). Collagenase-P was purchased from Roche (Basel, Basel-City, Switzerland). The following antibodies were used for flow cytometry: PE/Cyanine7 anti-mouse CD45 Antibody (103114), Brilliant Violet 605 anti-mouse/human CD11b Antibody (101257), Brilliant Violet 421 anti-mouse F4/80 antibody (123137), APC anti-mouse CD206 (MMR) antibody (141708), Alexa Fluor 488 anti-mouse Ly-6C antibody (128021) and PE anti-mouse CD192 C−C motif chemokine receptor 2 (CCR2) antibody (150609) from Biolegend (San Diego, CA, USA) and inducible nitric oxide synthase (iNOS) monoclonal antibody (CXNFT), PE from eBioscience (12-5920-80; Waltham, MA, USA).

2.2. Bacterial strains

Roseburia intestinalis DSM 14610 (*R. intestinalis*) was purchased from Mingzhou Biotechnology Co., Ltd. (Ningbo, China). *R. intestinalis* was cultured in Modified Reinforced Clostridial Broth for 48−72 h at 37 °C under anaerobic conditions. For further use, bacteria were subsequently collected by centrifugation at 8000×*g*

for 10 min (Centrifuge 5810R; Eppendorf, Hamburg, Germany) and resuspended in 200 μL phosphate buffer saline (PBS).

2.3. Animals and treatments

Male C57BL/6J mice (7−8 weeks old weighing 20 ± 2 g; JOINN Laboratories; Suzhou, China), *Tlr4*$^{-/-}$ C57BL/6J mice and littermate control wild-type mice (7−8 weeks old weighing 20 ± 2 g; Gempharmatech Co., Ltd.; Nanjing, China) were maintained in a specific pathogen-free environment at the Experimental Animal Center of Jiangnan University (Wuxi, China) with controlled temperature (24 ± 1 °C) and 12 h light/dark cycle and had free access to standard chow (Xietong Pharmaceutical Bio-engineering Co., Ltd.; Nanjing, China). All mice were adjusted to laboratory conditions 1 week before the experiments. All animal care and experimental protocols complied with the guidelines of and were approved by the Animal Ethics Committee of Jiangnan University (Approval Nos.: JN. No20180615c0500930 [97], JN. No20190915c0501208 [202], JN. No20191230c0900331 [375] and JN. No20221015c0501213 [438]).

CP was induced by repetitive caerulein injections. In brief, mice were given 6 intraperitoneal injections of caerulein (50 μg/kg body weight) per day at hourly intervals, 3 days per week, for a total of 4 weeks. Control mice were injected with vehicle saline. Mice were then sacrificed and analyzed on Day 3 after the last caerulein injection by a lethal dose of pentobarbital sodium. For the differentially targeted commensal bacterial disruption experiment, the mice were treated with broad-spectrum ABX (0.5 g/L vancomycin, 1 g/L neomycin, 1 g/L ampicillin, and 1 g/L metronidazole)[16], G^+ ABX (0.5 g/L vancomycin)[17] or G^- ABX (1 g/L neomycin)[18]. The mice were given antibiotics (200 μL/mouse) daily by gavage from a week before the caerulein injection to the sacrificed day. For the SCFA supplementation experiment, mice were treated with SCFA mix (67.5 mmol/L acetate, 40 mmol/L butyrate and 25.9 mmol/L propionate) in the drinking water and water solutions were changed daily[19]. For bacterial supplementation experiment, mice were orally administrated with *R. intestinalis* at a dose of 10^{10} colony forming units in 200 μL PBS/mice daily for 5 weeks. The experimental design of CP mice with different treatments was illustrated in Supporting Information Fig. S1.

2.4. Human samples

The recruitment of human subjects was approved by the ethics committee of Changhai Hospital Affiliated with The Second Military Medical University (CHEC2018-132). All subjects provided informed consent before participation and the experiments conformed to the principles set out in the WMA Declaration of Helsinki and the Department of Health and Human Services Belmont Report. CP patients presented with one of the conditions, including pancreatic calcification, moderate or severe pancreatic ductal changes, abnormal pancreatic function test, endoscopic ultrasound with signs of CP or histological change of CP as described by the Asia−Pacific consensus[20].

2.5. Histological analysis

Fresh pancreatic and colonic samples were fixed in 4% paraformaldehyde overnight, washed with running water for 2 h, rehydrated with gradient ethanol and then embedded in paraffin. The skiving machine slicer (Leica; Wetzlar, Hessen, Germany) diced 5 μm sections were stained with hematoxylin and eosin (H&E) or Masson's Trichrome (Sbjbio; Nanjing, China) following the standard procedures. The morphology evaluation was recorded by a digital slice scanner (3DHISTCH Ltd.; Budapest, Hungary). Pancreatic parenchymal rate is the area ratio of pancreas to the visual field, which represents the atrophic degree of the pancreas. Histological scoring of the colon according to the degree of shortening of the villi, 0: none, 1: mild, 2: moderate, 3: marked.

2.6. SCFA measurement

The SCFAs (acetate, propionate and butyrate), present in the colon content, were analyzed by gas chromatography-mass spectrometry as our previous reports[21]. Freeze-dried colon content (50 mg) was homogenized in 500 μL of saturated NaCl solution and then acidified with 40 μL 10% sulfuric acid. Diethyl ether of 0.8 mL was added to the sample to extract SCFAs. Samples were then centrifuged at 14,000 rpm for 15 min at 4 °C (Centrifuge 5810R; Eppendorf) and the supernatants were used for the analysis of the SCFAs. Supernatants were injected into Rtx-WAX capillary column (30 m × 0.25 mm × 0.25 μm; Shimadzu; Kyoto, Japan) installed on the GC and coupled to the MS detector of GCMS-QP2010 (Shimadzu). The initial oven temperature was 100 °C and increased to 140 °C at a rate of 7.5 °C/min. The temperature was further increased to 200 °C at a rate of 60 °C/min and remained for 3 min. Helium was utilized as the carrier gas at a flow rate of 0.89 mL/min and the column head pressure was 62.7 kPa. The injector was set at 240 °C. The injection mode was split and the ratio was 10:1. For the mass spectrometer, the ion source temperature was 220 °C, the interface temperature was 250 °C and the scan range was from *m/z* 2 to 100. Real-time analysis software GCMS Postrun (GCMS solution Version 2.72; Shimadzu) was employed to compare the relative concentrations of SCFAs.

2.7. Microbiota composition analysis

Total DNA was extracted from mouse colon content and human feces using the Fast DNA Spin Kit for Feces (MP Biomedicals; Shanghai, China) according to the manufacturer's instructions. The PCR amplification products were separated by 1% agarose gel electrophoresis and the Gel/PCR Extraction Kit (BIOMIGA; San Diego, CA, USA) was used to recover the target fragments. DNA was extracted from samples and the V3−V4 hypervariable region of the 16S rRNA gene was amplified and sequenced using the Illumina MiSeq platform. Taxonomies that were significantly enriched among different groups were identified by LEfSe using default settings. Other analyses including heatmaps and principal coordinates analysis plots were performed with internal scripts.

2.8. Gut permeability assay

For gut permeability assessment, 4 h fasted mice received 400 mg/kg FITC-dextran 4000 by gavage and blood was collected 4 h later. The serum concentration of FITC-dextran was determined by fluorometry (excitation 485 nm, emission 520 nm) on a microplate reader (FLUOstar Optima; BMG Labtech; Offenburg, Baden-Württemberg, Germany).

2.9. Enzyme-linked immunosorbent assays

Pancreatic monocyte chemoattractant protein-1 (MCP-1) level was measured with the Mouse CCL2/JE/MCP-1 Quantikine ELISA Kit from R&D System (Minneapolis, MN, USA) according to the protocols of the manufacturer. Absorbance was measured at 450 nm with a microplate reader Multiclan GO (Thermo Fisher Scientific). Pancreatic samples were homogenized in a saline solution (1:19, *w/v*). Samples were centrifuged at 4 °C, 10,000×*g* for 10 min (Centrifuge 5810R; Eppendorf). Protein concentrations were determined by a BCA Protein Assay Kit (Beyotime) during sample preparation to ensure that an equal amount of total protein was applied for cytokine measurements.

2.10. Quantification of mRNA by real-time quantitative PCR (RT-qPCR)

The mRNA levels for *Tgfb1*, *Col1*, *Acta2*, *Fn1*, *Camp*, *Defb1*, *Defb2*, *Reg1* and *Reg4* were analyzed by RT-qPCR. Total RNA was extracted from pancreatic tissues using TRIzol Reagent and was subjected to reverse transcription using a PrimeScript RT reagent Kit (TaKaRa Bio; Kyoto, Japan) following the instructions of the manufacturer. SYBR Green RT-qPCR was performed using the RT-qPCR system (Bio-Rad; Berkeley, CA, USA). The relative mRNA levels were normalized to mRNA levels of *Actb* (housekeeping control) and calculations for fold change of each mRNA were made on the comparative cycle threshold method ($2^{-\Delta\Delta Ct}$). The primers used in this study were provided in Table 1.

2.11. Immunofluorescence

The 5-μm thick tissue sections were cut from paraffin-embedded blocks. Antigen retrieval was performed for 30 min. Incubation with the anti-α-SMA antibody (1:200) was performed overnight at 4 °C. Secondary antibody incubation was performed for 1 h at room temperature. The DAPI staining was conducted according to the protocol provided by the manufacturer. Carl Zeiss microscope (Axio Vert A1; Jena, Thuringia, Germany) was used for the evaluation of immunofluorescence staining.

2.12. Flow cytometry

Freshly harvested pancreatic tissue samples were digested in 0.75 mg/mL collagenase-P solution at 37 °C for 15 min. Subsequently, tissue was homogenized in gentleMACS Dissociators (Miltenyi Biotec; Cologne, Bergisch Gladbach, Germany) and filtered through a 75-μm filter screen with PBS. Single-cell suspensions were incubated for 15 min at room temperature in PBS with the following antibodies: PE/Cyanine7 anti-mouse CD45, Brilliant Violet 605™ anti-mouse CD11b, Brilliant Violet 421™ anti-mouse F4/80, APC anti-mouse CD206 (MMR), Alexa Fluor® 488 anti-mouse Ly-6C, PE anti-mouse CCR2 and PE anti-mouse iNOS. Gating methods of fluorescence-activated cell sorting were programmed as $CD45^+CD11b^+Ly6C^{hi}CCR2^+$ for $CCR2^+$ monocytes (Supporting Information Fig. S2A), $CD45^+CD11b^+F4/80^+$ for macrophages, $CD45^+CD11b^+F4/80^+iNOS^+$ for M1 macrophages, $CD45^+CD11b^+F4/80^+CD206^+$ for M2 macrophages and $CD45^+CD11b^+F4/80^+CD206^+CCR2^+$ for $CCR2^+$ M2 macrophages (Fig. S2B). Stained cells were analyzed on an Attune NxT Flow Cytometer (Thermo Fisher Scientific) and data were analyzed using FlowJo software (BD Bioscience; Bergen County, NJ, USA).

2.13. Statistical analysis

The sample size declared in the different experimental groups was the number of independent mice in each group and statistical analysis was performed using these independent values. Data are expressed as mean with standard deviation (SD). For flow cytometry statistical analysis, data were expressed as median with interquartile range. $P < 0.05$ was considered statistically significant. Differences among three or more groups were determined using analysis of variance (ANOVA) followed by Tukey's *post hoc* test. All data were analyzed using GraphPad Prism 8 software (San Diego, CA, USA).

3. Results

3.1. Broad-spectrum ABX intensifies gut dysbiosis with decreased SCFAs-producing bacteria in CP

Several studies have demonstrated the association between gut dysbiosis and CP development. Patients and mice with CP both exhibit gut dysbiosis with decreased diversity and richness and taxa-composition changes[8,22–24]. Firstly, we examined how gut microbiota depletion by broad-spectrum ABX affected CP pathogenesis. As expected, the Shannon index revealed that the diversity of the intestinal microbiota was markedly decreased in mice with CP (Fig. 1A). Broad-spectrum ABX treatment further reduced the microbiota diversity (Fig. 1A). Moreover, the microbiota communities were remarkably different among control, CP and broad-spectrum ABX-treated CP mice (Fig. 1B). LEfSe analyses of the predominant microbial taxa confirmed altered microbial compositions among the three groups. CP mice

Table 1 Specific primers for RT-qPCR.

Gene	Forward	Reverse
Tgfb1	5′-CCCTATATTTGGAGCCTGGA-3′	5′-CTTGCGACCCACGTAGTAGA-3′
Col1	5′-GCTCCTCTTAGGGGCCACT-3′	5′-CCACGTCTCACCATTGGGG-3′
Acta2	5′-GTCCCAGACATCAGGGAGTAA-3′	5′-TCGGATACTTCAGCGTCAGGA-3′
Fn1	5′-ATGTGGACCCCTCCTGATAGT-3′	5′-GCCCAGTGATTTCAGCAAAGG-3′
Camp	5′-GCTGTGGCGGTCACTATCA-3′	5′-TGTCTAGGGACTGCTGGTTGA-3′
Defb1	5′-AGGTGTTGGCATTCTCACAAG-3′	5′-GCTTATCTGGTTTACAGGTTCCC-3′
Defb2	5′-CTGCTGCTGATATGCTGCCTC-3′	5′-TAAACTTCCAACAGCTGGAGTGG-3′
Reg1	5′-ATGGCTAGGAACGCCTACTTC-3′	5′-CCCAAGTTAAACGGTCTTCAGT-3′
Reg4	5′-GGCGTGCGGCTACTCTTAC-3′	5′-GGAAGTATCCATAGCAGTGGGA-3′
Actb	5′-AATCCCATCACCATCTTCCA-3′	5′-TGGACTCCACGACGTACTCA-3′

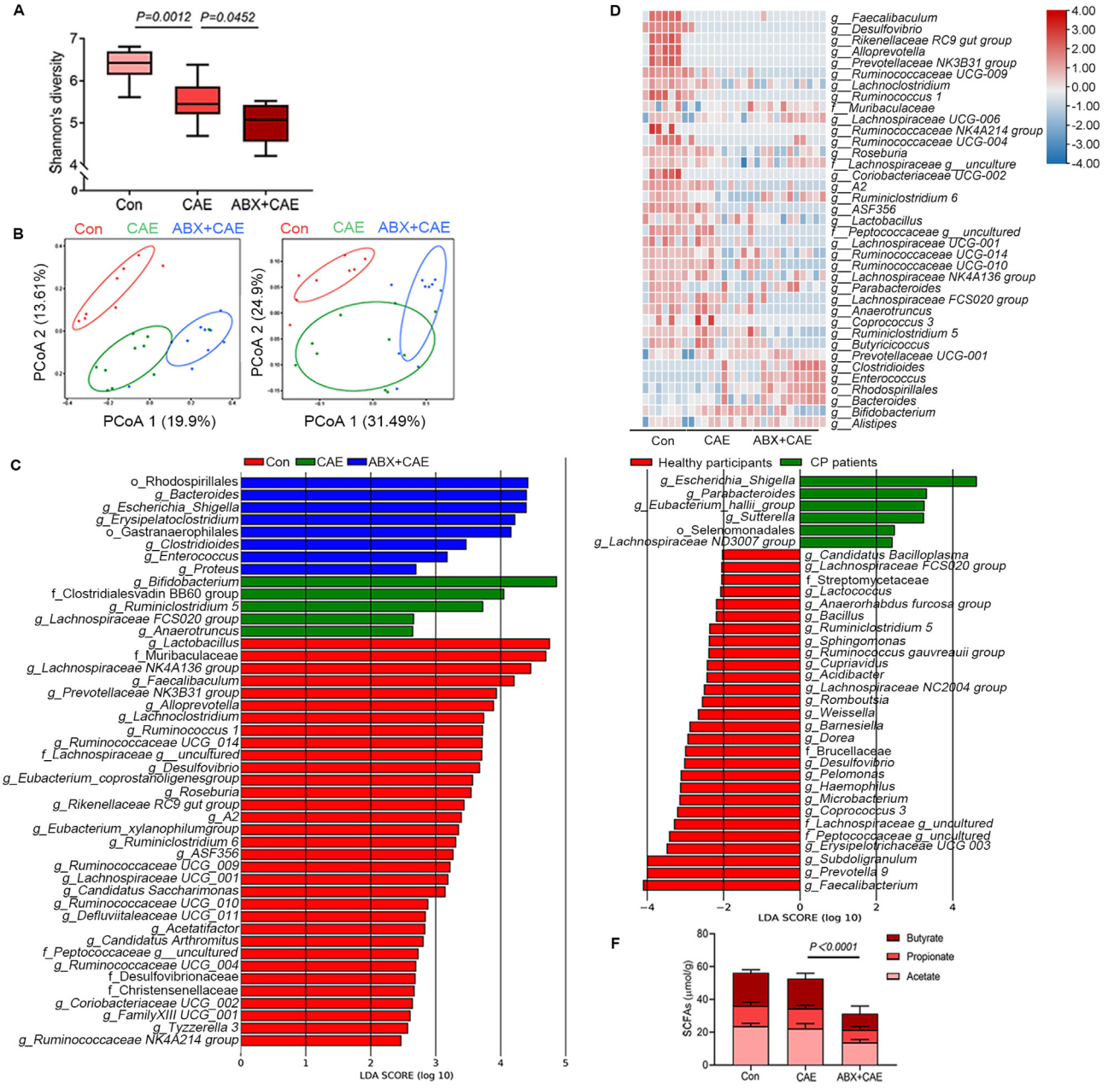

Figure 1 A broad-spectrum antibiotic (ABX) cocktail intensifies gut dysbiosis and reduction of short-chain fatty acids (SCFAs)-producing bacteria in chronic pancreatitis (CP). (A) The diversity shown by Shannon's index (Con, $n = 8$; CAE, $n = 10$; ABX + CAE, $n = 10$). (B) Principal coordinates analysis comparing the microbiome composition in colon content of mice (Con, $n = 8$; CAE, $n = 10$; ABX + CAE, $n = 10$; left: unweighted, right: weighted). (C) The LEfSe analyses of microbiome composition (based on abundance) distribution of three groups of mice, histogram of the LDA scores reveals the most differentially abundant taxa among different treatments (Con, $n = 8$; CAE, $n = 10$; ABX + CAE, $n = 10$). (D) Heatmap representation of SCFAs-producing bacteria (based on absolute count) in three groups of mice (Con, $n = 8$; CAE, $n = 10$; ABX + CAE, $n = 10$). (E) The LEfSe analyses of microbiome composition distribution of healthy participants and CP patients (healthy participants, $n = 69$; CP patients, $n = 71$). (F) The levels of SCFAs (acetate, propionate and butyrate) in colon content ($n = 6$). Data (A) were representative and were the min to the max from three independent experiments. Data (F) are representative and were the mean ± standard deviation (SD) from three independent experiments. *P* values were calculated by one-way analysis of variance (ANOVA) followed by Tukey's *post hoc* test for multiple comparisons.

and broad-spectrum ABX-treated CP mice exhibited remarkably reduced compositions of the preferential microbial taxa, compared with the control group (Fig. 1C). Interestingly, the predominant microbial taxa in control mice were mostly SCFAs-producers, which were significantly reduced in CP mice and broad-spectrum ABX-treated CP mice (Fig. 1C and Supporting Information Fig. S3, Tables S1 and S2). These results were further evidenced by heatmap analysis of SCFAs-producers in the three groups of mice (Fig. 1D). Compared with control mice, CP mice and broad-spectrum ABX-treated CP mice displayed reduced

abundances of predominant SCFAs-producers, especially SCFAs-producing G^+ bacteria, including *Ruminococcus 1*, *Ruminococcaceae UCG-009*, *Peptococcaceae*, *Lachnospiraceae UCG-001*, *Lactobacillus*, *Roseburia* and *Lachnoclostridium*, with a more pronounced effect observed in ABX-treated CP mice (Fig. 1D). LEfSe analyses of the fecal microbiota of 69 healthy participants and 71 CP patients showed that the abundance of SCFAs-producing bacteria was significantly decreased in CP patients compared with healthy participants, especially SCFAs-producing G^+ bacteria, including *Faecalibacterium*, *Subdoligranulum*, *Peptococcaceae* and *Lachnospiraceae* (Fig. 1E and Supporting Information Table S3). These changes were consistent with what was observed in CP mice. Given that SCFAs-producing bacteria were primarily affected during disease progression, we next examined the levels of colonic SCFAs in different groups. Not surprisingly, depletion of predominant SCFAs-producing bacteria in broad-spectrum ABX-treated CP mice was accompanied by decreased levels of colonic SCFAs (acetate, propionate and butyrate) (Fig. 1F). Collectively, broad-spectrum ABX treatment aggravates gut dysbiosis and importantly decreases the abundance of SCFAs-producing commensal bacteria in mice with CP.

3.2. *Broad-spectrum ABX treatment aggravates the severity of CP*

Next, we examined how microbiota depletion by broad-spectrum ABX affected the development of CP. Broad-spectrum ABX worsened pancreatic atrophy and weight loss, which are symptomatic characteristics of CP (Fig. 2A and B). Histological examination of pancreatic sections also confirmed an overall aggravated index of disease severity after broad-spectrum ABX treatment (Fig. 2C). Pancreatic atrophy and/or fibrosis cause the irreversible destruction of pancreatic parenchyma[25]. CP induction significantly decreased pancreatic parenchyma rate and broad-spectrum ABX further exacerbated the condition (Fig. 2C). Pancreatic fibrosis is a hallmark of CP and contributes to gradual pancreatic insufficiency and is majorly associated with the activation of PSCs[25,26]. Next, we demonstrated that the mRNA expression of profibrotic growth factors *Tgfb1*, *Col1*, *Acta2* and *Fn1* in the pancreas was highly induced by broad-spectrum ABX treatment compared with the untreated CP group (Fig. 2D). To determine the extent of fibrosis, sections were evaluated by Masson's Trichrome staining, which preferentially labels collagen fibrils with blue color[27]. Depletion of commensal bacteria aggravated the deposition of collagen fibers in CP (Fig. 2E), which was accompanied by upregulation of α-SMA in the pancreas (Fig. 2F). Together, these results show that microbiota depletion caused by broad-spectrum ABX exacerbates the severity of CP.

3.3. *Depletion of G^+ bacteria but not G^- bacteria diminishes SCFAs-producing G^+ bacteria and aggravates the severity of CP*

To further reveal the effect of different commensal bacteria on the development of CP, we further applied vancomycin to deplete G^+ bacteria and neomycin to eliminate G^- bacteria. LEfSe analyses of microbiome composition revealed that both G^+ ABX and G^- ABX impacted the relative abundances of SCFAs-producing bacteria (Supporting Information Fig. S4 and Table S4). Heatmap representation of distributions of SCFAs-producers in four different groups further showed that G^- ABX significantly decreased the relative abundances of SCFAs-producing G^- bacteria *Bacteroides*[28] and Rhodospirillales[29] (Fig. 3A). G^+ ABX significantly reduced the abundances of SCFAs-producing G^+ bacteria including *Ruminococcus 1*, *Ruminococcaceae UCG-009*, *Peptococcaceae*, *Lachnospiraceae UCG-001*, *Lactobacillus*, *Roseburia* and *Lachnoclostridium* (Fig. 3A). Both G^- ABX and G^+ ABX caused significant decreases in SCFA levels, with a more pronounced effect observed for G^+ ABX (Fig. 3B). However, only G^+ ABX further aggravated CP-associated intestinal barrier damage (Supporting Information Fig. S5).

G^+ ABX but not G^- ABX further aggravated pancreatic atrophy (Fig. 3C) and pancreatic weight loss (Fig. 3D). Additionally, depletion of G^+, but not G^- bacteria exaggerated typical features of CP, as evidenced by an increased index of disease severity (Fig. 3E), pancreatic fibrosis (Fig. 3F and G) and the activation of PSCs (Fig. 3H). Collectively, these results show that disruption of G^+ bacteria accelerates the severity of CP, pointing to a critical role of SCFAs-producing G^+ bacteria.

3.4. *Toll-like receptor 4 (TLR4) signaling is not involved in G^+ ABX-induced exacerbation of CP*

TLR4 is the receptor of lipopolysaccharide and plays a vital role in mediating the effects of G^- bacteria[30]. We therefore investigated whether TLR4 is involved in G^+ ABX-induced exacerbation of CP by using TLR4 knockout mice ($TLR4^{-/-}$ mice). The results showed no difference in intestinal permeability (Fig. 4A), pancreatic atrophy (Fig. 4B), pancreatic weight loss (Fig. 4C), pancreatic histology (Fig. 4D) and pancreatic fibrosis (Fig. 4E and F) in $TLR4^{-/-}$ mice following CP induction compared with their wild type (WT) controls. Activated PSCs exacerbate CP by secreting large amounts of MCP-1 to recruit its C−C Motif chemokine receptor 2 (CCR2)-positive inflammatory monocytes from peripheral blood to the pancreas[31,32]. Therefore, next, we examined the expression of MCP-1 and proportions of plasma monocytes and pancreatic macrophages. Compared with control mice, the expression of pancreatic MCP-1 and the populations of $CCR2^+$ monocytes were significantly increased in G^+ ABX-treated $TLR4^{-/-}$ and WT with CP (Fig. 4G and Supporting Information Fig. S6A). As a key cell type involved in pancreatic fibrosis, the activation of PSCs facilitates the activation of M2 macrophage polarization and CP progression[15]. Herein, we found significantly enhanced frequencies of pancreatic macrophages, M1 macrophages, M2 macrophages and $CCR2^+$ M2 macrophages both in ABX-treated $TLR4^{-/-}$ and WT mice with CP (Fig. S6B−S6E). Meanwhile, the deletion of TLR4 had no effect on G^+ ABX-exacerbated immune disorders in CP. Collectively, the data suggest that TLR4 is not involved in mediating the worsening of CP caused by G^+ ABX.

3.5. *SCFAs rebuild the barrier function and protect CP*

Altered gut microbiota composition has been reported to be associated with alterations in gut barrier integrity in patients with CP[33]. As inducers of intestinal antimicrobial peptides, SCFAs have been shown to indirectly regulate gut barrier[34]. Thus, we next explored whether SCFA supplementation could improve intestinal barrier function and protect CP.

Our data show that SCFAs improved the colonic damage caused by CP (Supporting Information Fig. S7A). Importantly, compared with CP mice, SCFA supplementation enhanced the expression of *Camp*, *Defb1* and *Defb2*, while decreasing the expression of *Reg1* and *Reg4* (Fig. S7B). These antimicrobial

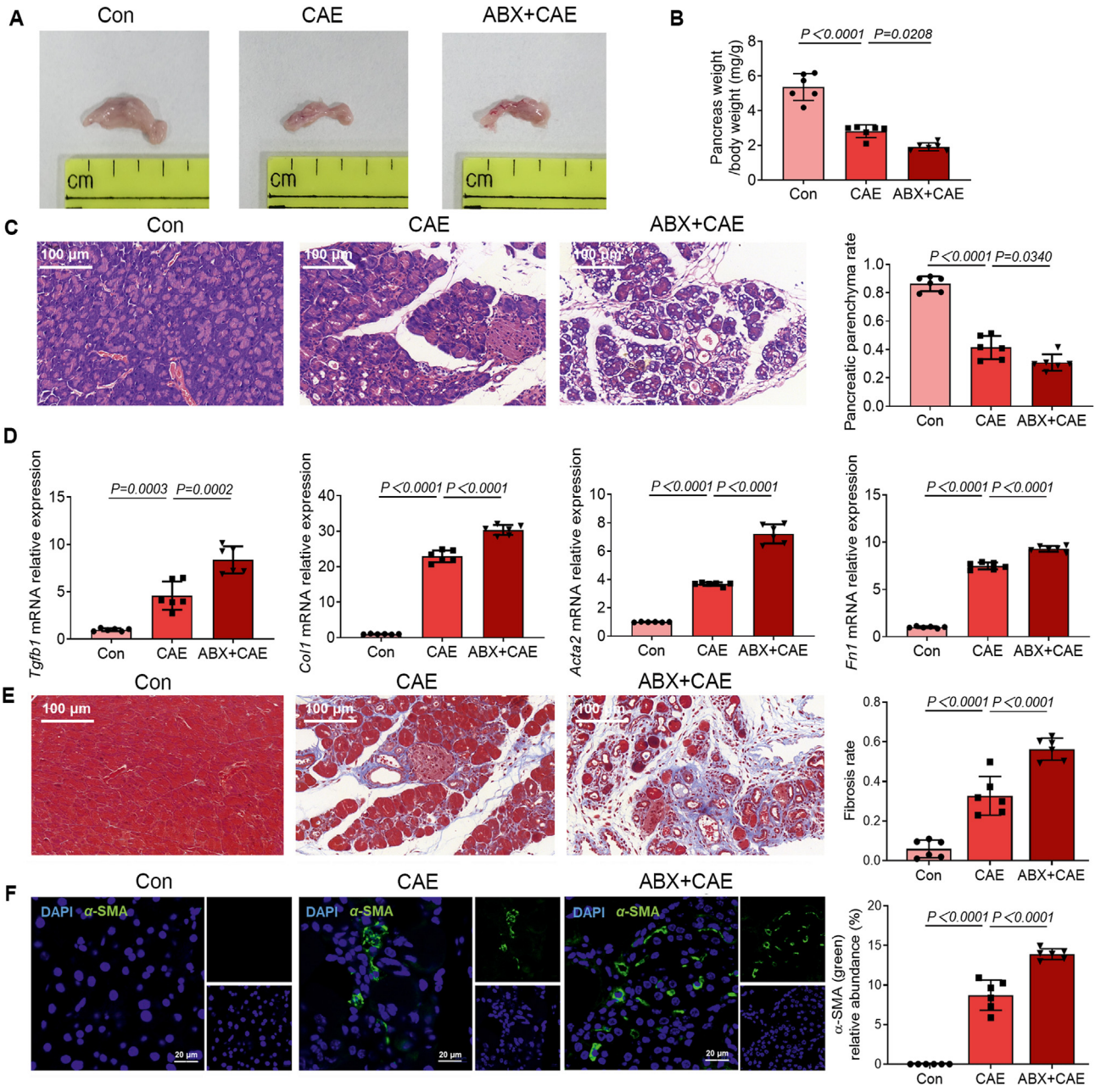

Figure 2 A ABX cocktail aggravates CP. (A) The representative macrographic images of the pancreas. (B) The ratio of pancreatic weight and body weight ($n = 6$). (C) The representative images and parenchyma rates of the pancreas by hematoxylin and eosin (H&E) staining ($n = 6$). Scale bar: 100 μm. (D) The fibrosis-associated gene (*Tgfb1*, *Col1*, *Acta2* and *Fn1*) expression in the pancreas ($n = 6$). (E) The representative images and fibrosis rates of the pancreas by Masson's Trichrome staining ($n = 6$). Scale bar: 100 μm. (F) Localization and expression of α-smooth muscle actin (α-SMA) (green) in the pancreas by immunofluorescent staining ($n = 6$). Representative photomicrographs of individual and merged staining were shown. Nuclei were stained with 4′,6-diamidino-2-phenylindole (DAPI) (blue). Scale bar: 20 μm. Data (B−F) are representative and were the mean ± SD from three independent experiments. *P* values were calculated by one-way ANOVA followed by Tukey's *post hoc* test for multiple comparisons.

peptides have been proved to regulate gut barrier function and host immune responses[16,35]. Meanwhile, the severity of CP was inhibited by SCFA supplementation as evidenced by increased pancreas weight and alleviated pancreatic fibrosis (Fig. S7C−S7E). Notably, the depletion of G^+ bacteria intensified CP, accompanied by gut barrier dysfunction (Fig. 5A−C). SCFA supplementation relived gut barrier damage caused by G^+ ABX treatment (Fig. 5A−C). Besides, pancreatic atrophy and pancreas weight loss caused by the depletion of G^+ bacteria were attenuated by exogenous SCFA supplementation (Fig. 5D−F). Not only pancreatic fibrosis, but also the activation of PSCs was alleviated by SCFA supplementation (Fig. 5G and H). Together, SCFA supplementation improves gut barrier dysfunction in CP mice and has a protective effect on CP.

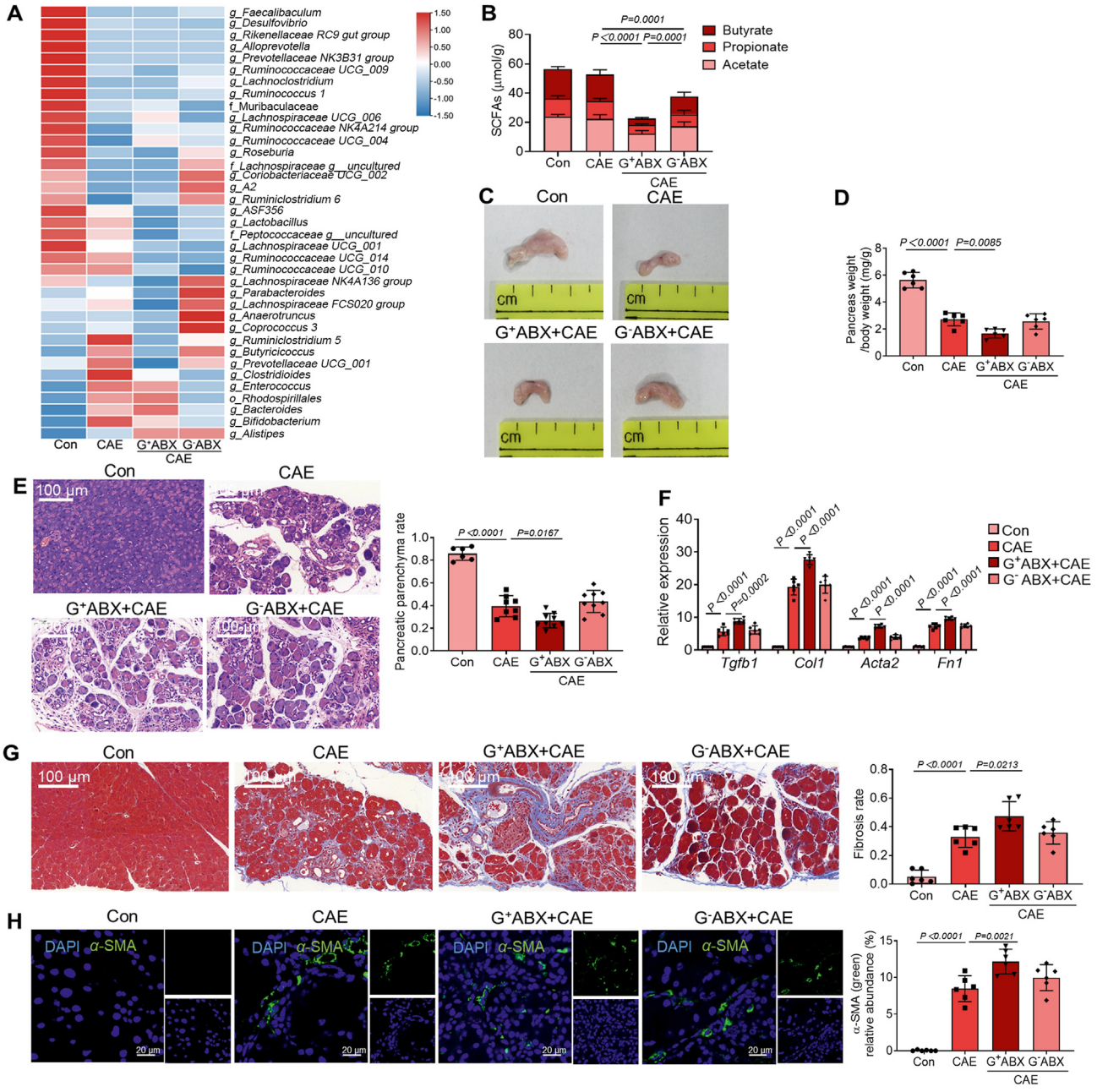

Figure 3 Depletion of Gram-positive bacteria causes decreased abundances of SCFAs-producing Gram-positive bacteria and intensifies CP. (A) Heatmap representation of SCFAs-producing bacteria in four groups of mice. (Con, $n = 8$; CAE, $n = 10$; G^+ ABX+CAE, $n = 10$; G^- ABX + CAE, $n = 10$). (B) SCFA concentrations (acetate, propionate and butyrate) in colon content ($n = 6$). (C) The representative macrographic images of the pancreas. (D) The ratio of pancreatic weight and body weight ($n = 6$). (E) The representative images and parenchyma rates of the pancreas by H&E staining ($n = 6$). Scale bar: 100 μm. (F) The fibrosis-associated gene (*Tgfb1*, *Col1*, *Acta2* and *Fn1*) expression in the pancreas ($n = 6$). (G) The representative images and fibrosis rates of the pancreas by Masson's Trichrome staining ($n = 6$). Scale bar: 100 μm. (H) Localization and expression of α-SMA (green) in the pancreas by immunofluorescent staining ($n = 6$). Representative photomicrographs of individual and merged staining were shown. Nuclei were stained with DAPI (blue). Scale bar: 20 μm. Data (B, D–H) were representative and were the mean ± SD from three independent experiments. *P* values were calculated by one-way ANOVA followed by Tukey's *post hoc* test for multiple comparisons.

3.6. SCFAs alleviate monocyte recruitment and pancreatic macrophage deregulation in mice with CP

Accumulating studies have reported the crucial roles of SCFAs in regulating immune cell responses[36,37]. We previously confirmed that exogenous SCFAs could alleviate the symptoms of CP in mice (Fig. 5). However, the mechanisms underlying the protective effects of SCFAs on CP mice remain unclear. In this context, we examined how SCFAs regulate the recruitment of monocytes and the infiltration and polarization of pancreatic macrophages of CP

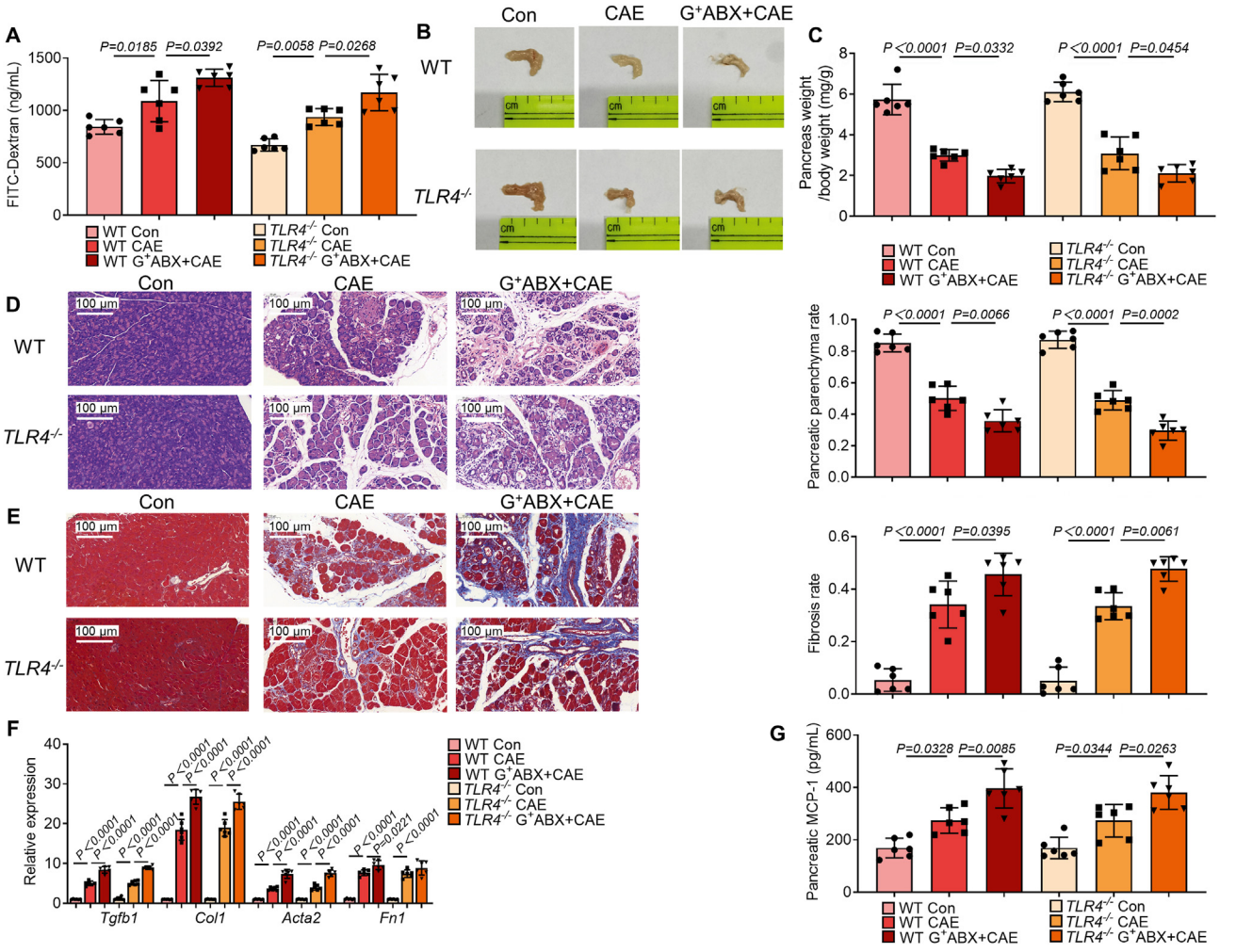

Figure 4 Toll-like receptor 4 (TLR4) deficiency does not influence the severity of CP. (A) Intestinal permeability was assessed by measuring fluorescein isothiocyanate (FITC)-dextran ($n = 6$). (B) The representative macrographic images of the pancreas. (C) The ratio of pancreatic weight and body weight ($n = 6$). (D) The representative images and parenchyma rates of the pancreas by H&E staining ($n = 6$). Scale bar: 100 μm. (E) The representative images and fibrosis rates of the pancreas by Masson's Trichrome staining as indicated by collagen-rich scars (blue color) ($n = 6$). Scale bar: 100 μm. (F) The fibrosis-associated gene (*Tgfb1*, *Col1*, *Acta2* and *Fn1*) expression in the pancreas ($n = 6$). (G) The monocyte chemoattractant protein-1 (MCP-1) levels in the pancreas ($n = 6$). Data (A, C–G) are representative and were the mean ± SD from three independent experiments. *P* values were calculated by one-way ANOVA followed by Tukey's *post hoc* test for multiple comparisons.

mice treated with G^+ ABX. The expression of MCP-1, the populations of $CCR2^+$ monocytes, macrophages, M1 macrophages, M2 macrophages and $CCR2^+$ M2 macrophages were all enhanced in CP mice (Fig. 6A–F). Moreover, the expression of pancreatic MCP-1, the recruitment of monocytes and macrophage infiltration and polarization in CP were potentiated by G^+ ABX treatment, but alleviated by SCFA supplementation (Fig. 6A–F). Collectively, the recruitment of $CCR2^+$ monocytes, the infiltration of inflammation-associated M1 macrophages, fibrosis-associated M2 macrophages and $CCR2^+$ M2 macrophages are accumulated in mice with CP and G^+ ABX-treated CP mice and exogenous SCFAs treatment significantly alleviates the condition.

3.7. *Supplementation of SCFAs-producing G^+ bacteria alleviates CP*

Our previous results indicate an essential role of G^+ SCFAs-producing bacteria in the prevention or treatment of CP. Finally, we performed an *in vivo* experiment to verify their effects in CP mice. Herein, the available isolated strain *Roseburia intestinalis* DSM 14610 (*R. intestinalis*) of the G^+ SCFAs-producer *Roseburia* that were significantly decreased in CP mice, broad-spectrum ABX-treated CP mice and G^+ ABX-treated CP mice was chosen[38]. Not surprisingly, *R. intestinalis* treatment significantly enhanced the colonic SCFA content and alleviated CP-associated intestinal barrier dysfunction (Fig. 7A–C). Accordingly, the expression levels of colonic antimicrobial peptides including *Camp*, *Defb1*, *Defb2* were increased and *Reg1* and *Reg4* were decreased after treatment with *R. intestinalis* (Fig. 7D). In addition, *R. intestinalis* treated CP mice exhibited alleviated pancreatic atrophy and weight loss (Fig. 7E and F). Importantly, *R. intestinalis* attenuated pancreatic injury and fibrosis caused by CP, as marked by improved pancreatic histological damage, and reduced the extent of fibrosis of pancreatic sections and mRNA expression of fibrosis markers (Fig. 7G–I). Together, our results support that treatment with SCFAs-producing G^+ bacteria can relieve the severity of CP.

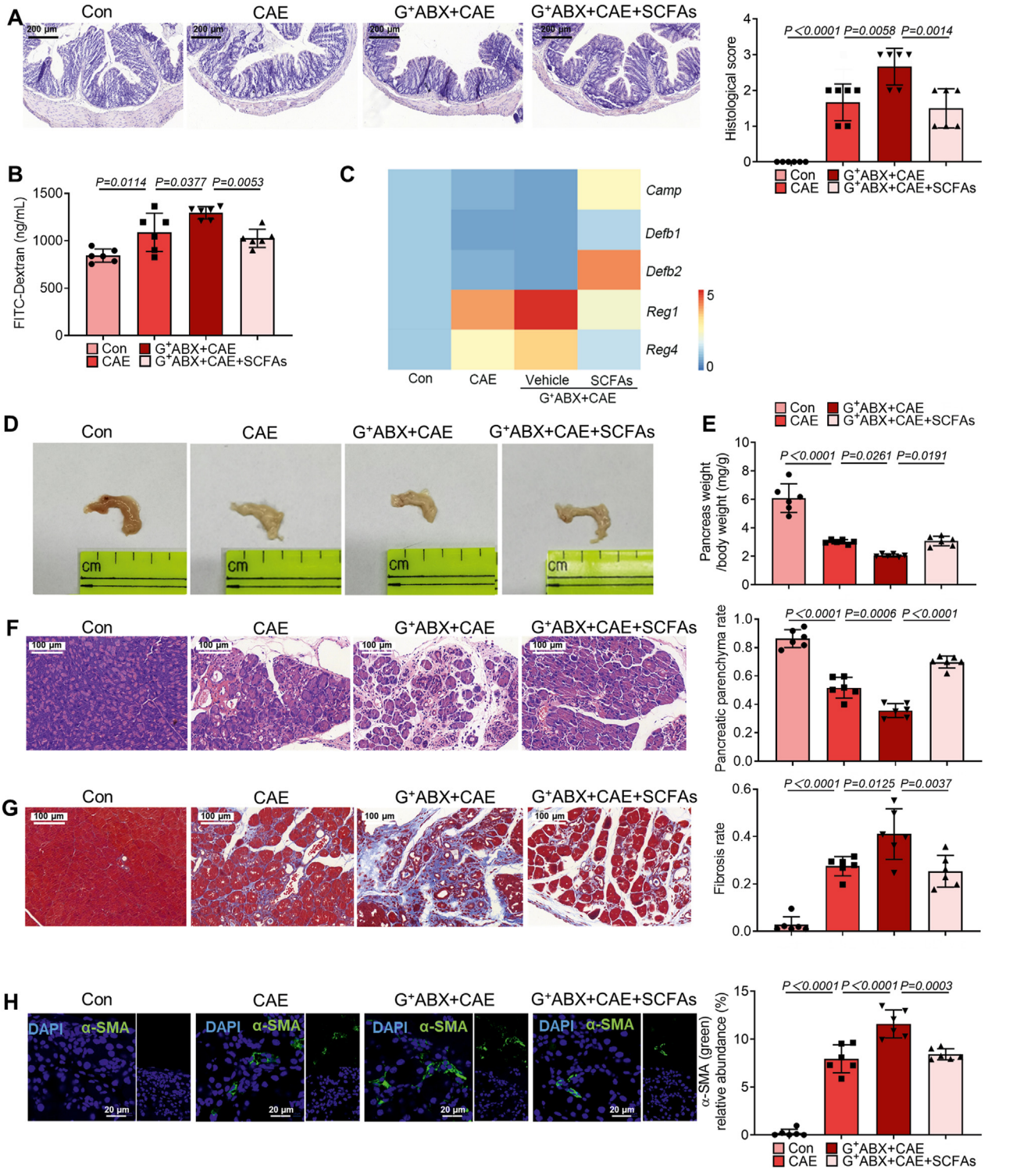

Figure 5 SCFAs mitigate the intensified effects of the depletion of Gram-positive bacteria on CP. (A) The representative images and histological scores of the colon by H&E staining ($n = 6$). Scale bar: 200 μm. (B) Intestinal permeability assessment by measuring FITC-dextran ($n = 6$). (C) The mRNA expression of antimicrobial peptides (*Camp*, *Defb1*, *Defb2*, *Reg1* and *Reg4*, $n = 6$). (D, E) The representative macroscopic images of the pancreas (D) and the ratio of pancreatic weight and body weight (E) ($n = 6$). (F) The representative images and parenchyma rates of the pancreas by H&E staining ($n = 6$). Scale bar: 100 μm. (G) The representative images and fibrosis rates of the pancreas by Masson's Trichrome staining ($n = 6$). Scale bar: 100 μm. (H) Localization and expression of α-SMA (green) in the pancreas by immunofluorescent staining ($n = 6$). Representative photomicrographs of individual and merged staining were shown. Nuclei were stained with DAPI (blue). Scale bar: 20 μm. Data are representative and were the mean ± SD from three independent experiments. *P* values were calculated by one-way ANOVA followed by Tukey's *post hoc* test for multiple comparisons.

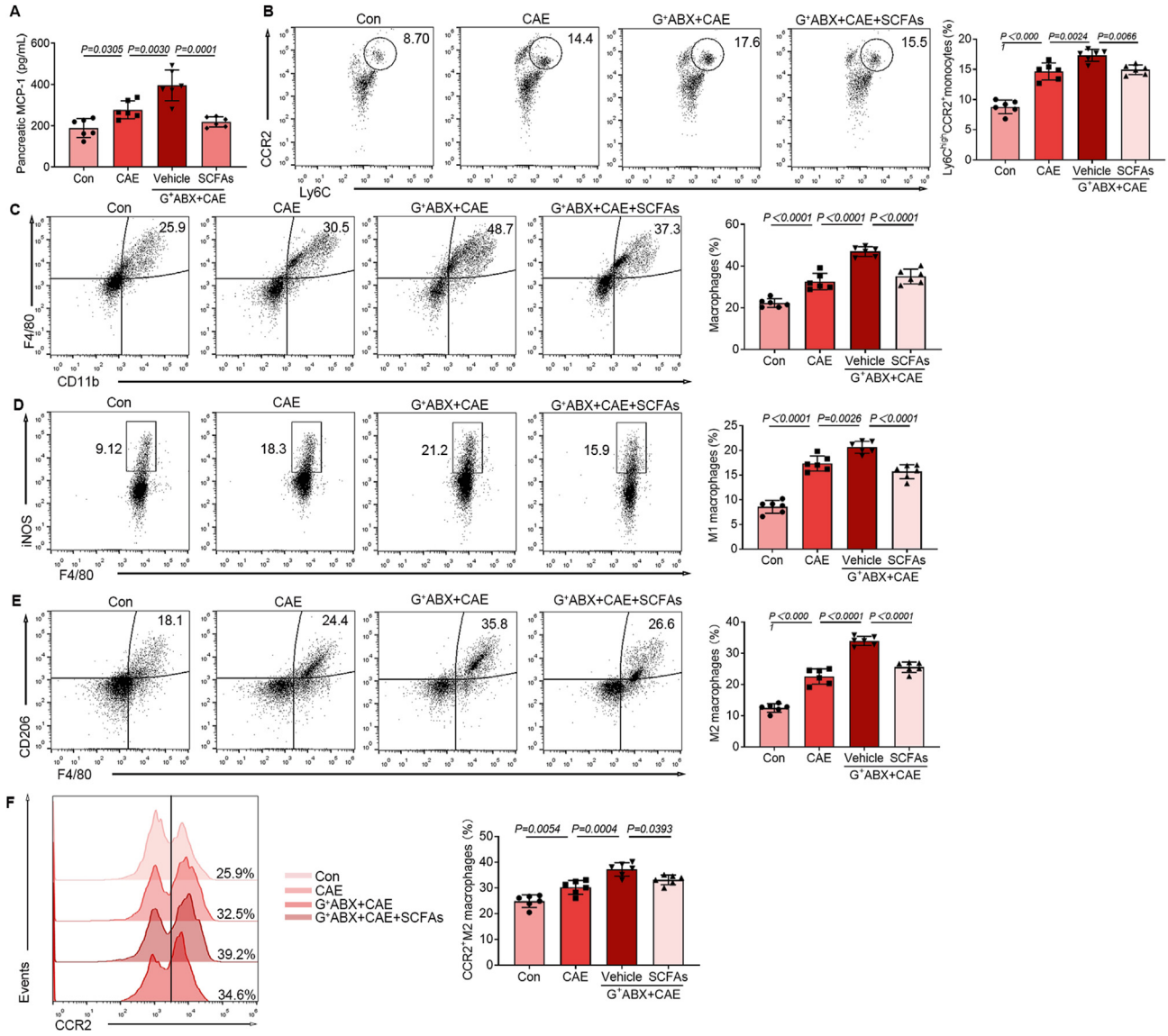

Figure 6 SCFAs alleviate monocyte recruitment and pancreatic macrophage deregulation in mice with CP. (A) The MCP-1 levels in the pancreas ($n = 6$). (B) The frequency of Ly6C^{hi} C−C Motif chemokine receptor 2 (CCR2)$^+$ monocytes among CD45$^+$CD11b$^+$ population ($n = 6$). (C) The frequency of CD11b$^+$F4/80$^+$ macrophages among CD45$^+$ population ($n = 6$). (D) The frequency of inducible nitric oxide synthase (iNOS)$^+$ M1 macrophages among CD45$^+$CD11b$^+$F4/80$^+$ population ($n = 6$). (E) The frequency of F4/80$^+$CD206$^+$ M2 macrophages among CD45$^+$CD11b$^+$ population ($n = 6$). (F) The frequency of CCR2$^+$ M2 macrophages among CD45$^+$CD11b$^+$ F4/80$^+$CD206$^+$ population ($n = 6$). Data (A) are representative and were the mean ± SD from three independent experiments. Data (B−F) were representative and were the median ± interquartile range from three independent experiments. *P* values were calculated by one-way ANOVA followed by Tukey's *post hoc* test for multiple comparisons.

4. Discussion

Our study demonstrates that gut dysbiosis in particular depletion of SCFAs-producing bacteria promotes the progression of CP. Disruption of G$^+$ bacteria decreases the levels of SCFAs and compromises gut barrier function, which results in aggravated pancreatic fibrosis, monocyte recruitment and M2 macrophage polarization. SCFA supplementation improves intestinal barrier dysfunction and alleviates monocyte recruitment and pancreatic macrophage deregulation, thereby protecting against the development of CP.

A healthy and stable gut microbiota community is vital in maintaining homeostatic balance and metabolism[39]. The imbalance of gut microbiota or called gut dysbiosis has recently been found to be associated with pathogenesis of many diseases including CP[8]. A potential role of gut dysbiosis in progression of CP has, however, not been clearly demonstrated. To establish a causal role of alterations to the gut microbial community composition in the development of CP, we applied a broad-spectrum antibiotic cocktail to disturb the microbial community in mice with CP. Notably, broad-spectrum ABX treatment intensified gut dysbiosis, in particular decreased abundances of SCFAs-producing bacteria, including *Ruminococcus 1*,

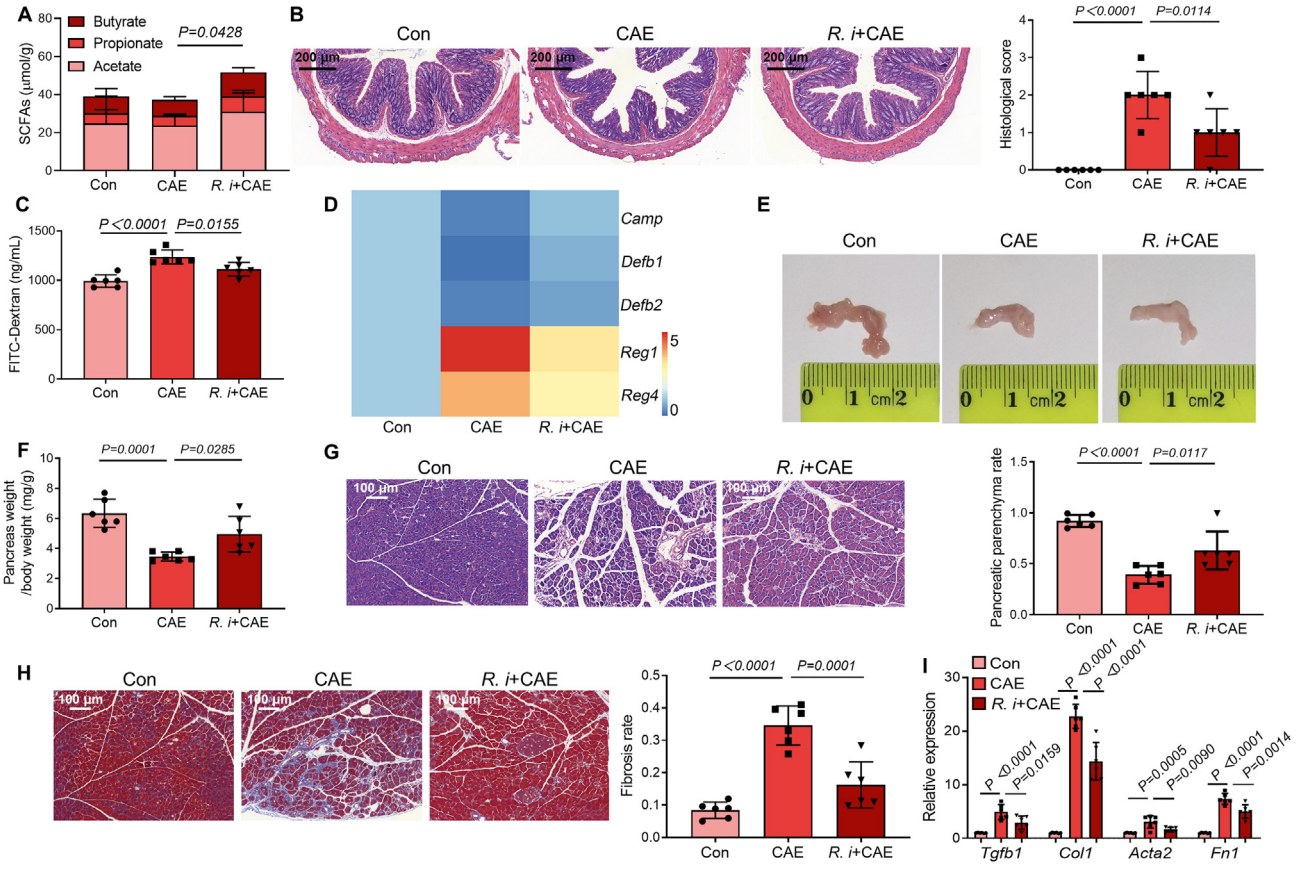

Figure 7 Oral treatment with a specific G^+ SCFAs-producer *Roseburia intestinalis* (*R. intestinalis*) attenuates the severity of CP. (A) The levels of SCFAs (acetate, propionate and butyrate) in colon content ($n = 6$). (B) The representative images and histological scores of the colon by H&E staining ($n = 6$). Scale bar: 200 μm. (C) Intestinal permeability assessment by measuring FITC-dextran ($n = 6$). (D) The mRNA expression of antimicrobial peptides (*Camp*, *Defb1*, *Defb2*, *Reg1* and *Reg4*, $n = 6$). (E, F) The representative macroscopic images of the pancreas (E) and the ratio of pancreatic weight and body weight (F) ($n = 6$). (G) The representative images and parenchyma rates of the pancreas by H&E staining ($n = 6$). Scale bar: 100 μm. (H) The representative images and fibrosis rates of the pancreas by Masson's Trichrome staining ($n = 6$). Scale bar: 100 μm. (I) The mRNA expression of markers relevant to pancreatic fibrosis ($n = 6$). Data (A–D and F–I) are representative and were the mean ± SD from three independent experiments. *P* values were calculated by one-way ANOVA followed by Tukey's *post hoc* test for multiple comparisons.

Ruminococcaceae UCG-009, *Peptococcaceae*, *Lachnospiraceae UCG-001*, *Lactobacillus*, *Roseburia* and *Lachnoclostridium*. These bacteria have demonstrated beneficial effects on human health and immune system[40]. All these findings suggest that SCFAs-producing bacteria may play a critical role in the progression of CP. To further specify these SCFAs-producing bacteria, we next used ABX targeting the disruption of G^+ or G^- bacteria. We observed that G^+ ABX treatment exacerbated the CP development, as evidenced by aggravated pancreatic fibrosis, monocyte recruitment, pancreatic macrophage deregulation, gut dysbiosis and the depletion of SCFAs-producing G^+ bacteria. Importantly, G^+ ABX diminished major SCFAs-producing G^+ bacteria including *Ruminococcus 1*, *Ruminococcaceae UCG-009*, *Peptococcaceae*, *Lachnospiraceae UCG-001*, *Lactobacillus*, *Roseburia* and *Lachnoclostridium*, resulting in significantly decreased SCFA production and disruption of barrier integrity, contributing to the overall worsening effect on CP development. In contrast, although G^- ABX caused depletion of SCFAs-producing G^- bacteria *Bacteroides* and Rhodospirillales, its effects on gut barrier dysfunction were insignificant, which was in agreement with its overall non-effect on CP progression.

CP is a disease characterized by malabsorption and impaired exocrine pancreatic function, accompanied by altered intestinal microbiota composition, as marked by depletion of anaerobes and significant enrichment of G^- and opportunistic pathogenic bacteria (such as *Bacteroides* and *Prevotella*)[41]. Intriguingly, as the receptor of lipopolysaccharide, TLR4 deficiency in G^+ ABX-treated mice did not influence CP, suggesting that mechanisms other than *via* TLR4 may play a part in the pathogenesis of CP. In addition, among G^- SCFAs-producers, both barrier-protective species (*Bacteroides fragilis*, *Bacteroides vulgatus* and *Bacteroides dorei*) from genera *Bacteroides* and barrier-damaging species (*Prevotella intestinalis*, *Prevotella histicola* and *Prevotella copri*) from genera *Prevotella* have been reported[42–46], which explained the end outcome of G^- ABX treatment on CP.

Given that SCFAs-producing G^+ bacteria were critically involved in the development of CP, we next addressed whether SCFAs could alleviate CP. Indeed, SCFA supplementation protected intestinal barrier integrity, attenuated CP-associated monocyte recruitment, pancreatic macrophage deregulation and pancreatic fibrosis, thus protecting the development of CP. The protective effects of SCFAs are associated with upregulated expressions of *Camp* and *Defb2* and downregulated expressions of *Reg1* and *Reg4*. The antimicrobial peptides cathelicidin-related antimicrobial peptide and defensin beta-2 contribute to the

antimicrobial barrier function of the intestinal mucosa[47,48]. In contrast, REG proteins are constitutively synthesized by pancreatic acinar cells and upregulated dramatically during acute pancreatic inflammation[49]. Accordantly, we observed that downregulated expressions of *Reg1* and *Reg4* were associated with alleviated inflammation caused by SCFA supplementation. SCFAs are microbially produced metabolites, as crucial executors of diet-based microbial influence on the host. By binding to the G-protein-coupled receptors, they exert profound effects on inflammatory responses[50,51]. Also, SCFAs have been reported with multiple functions including regulating gut microbiota composition and inducing the production of antimicrobial peptides[34,52]. Previous reports showed that phytochemicals such as curcumin targeting PSCs as potential anti-fibrotic agents for CP[53]. Intriguingly, supplementation with curcumin could also enhance the abundance of SCFAs-producing bacteria and SCFA content in the mouse colon[54]. These findings imply that targeting SCFAs maybe a potential solution for CP therapy.

Accordingly, herein, our study found that administration of SCFAs not only improved CP-associated gut barrier dysfunction, but also alleviated the infiltration and polarization of macrophages by decreasing the recruitment of $CCR2^+$ monocytes in G^+ ABX-treated CP mice.

Macrophages can be divided into two spectra of major types: M1, which are correlated with inflammation; and M2, which are dominant in mouse and human CP[15]. M2 macrophages have been observed in close proximity to PSCs and promote pancreatic fibrosis in CP[15]. Activated PSCs can secrete MCP-1, which further promotes the recruitment of monocytes and the infiltration and polarization of macrophages into pancreatic microenvironment[31]. Macrophages enter the pancreas in response to an upregulated level of the chemokine MCP-1 acting on the macrophage receptor CCR2[55]. Thus, CCR2/MCP-1 axis-mediated monocyte migration and M2 macrophage polarization in the pancreas are critically involved in CP[56]. These responses were exacerbated by G^+ ABX-treatment and were significantly alleviated by SCFA supplementation. Similar to SCFA supplementation, specific SCFAs-producing G^+ bacteria (*i.e.*, *R. intestinalis*) treatment also significantly attenuated the severity of CP. These intriguing findings further indicated a critical role of SCFAs-producing G^+ bacteria and SCFAs in CP development. Consequently, our data support the supplementation of a combined SCFAs-producing G^+ bacteria or SCFAs in the management of CP.

5. Conclusions

Our study demonstrates, for the first time, a critical role of SCFAs-producing G^+ bacteria in maintaining intestinal barrier, regulating monocyte/macrophage homeostasis and pancreatic fibrosis. Depletion of G^+ bacteria contributes to decreased levels of SCFAs, intensified intestinal barrier dysfunction and monocyte/macrophage deregulation, thereby aggravating the progression of CP. In summary, our study points to the potential therapeutic interventions of dietary-derived SCFAs or targeting SCFAs-producing G^+ bacteria in the prevention or treatment of CP.

Acknowledgments

The authors greatly acknowledge Prof. Xiaoyan Wang from the Third Xiangya Hospital, Central South University for intellectual input. The study was supported by funds from the National Natural Science Foundation of China (Grant Nos. 82070666 and 82122068), the Natural Science Foundation for Distinguished Young Scholars of Jiangsu Province (Grant No. BK20200026, China), the Collaborative Innovation Center of Food Safety and Quality Control of Jiangsu Province, the Fundamental Research Funds for the Central Universities (Grant Nos. JUSRP221037 and JUSRP22007, China), the China Postdoctoral Science Foundation (Grant No. 2022M721366), the Excellent Postdoctoral Program of Jiangsu Province (Grant No. 2023ZB168, China), Wuxi City's first "double hundred" young and middle-aged medical and health talents (Grant No: BJ2020045, China) and Wuxi Social Development Science and Technology Demonstration Project (Grant No: N20201003, China).

Author contributions

Li-Long Pan, Zheng-Nan Ren, Jun Yang and Bin-Bin Li: conceptualization, methodology, investigation, validation, writing-original draft and writing-reviewing and editing. Yi-Wen Huang, Dong-Xiao Song, Xuan Li and Jia-jia Xu: methodology and investigation. Madhav Bhatia: writing-reviewing and editing. Duo-Wu Zou and Chun-Hua Zhou: methodology and resources. Jia Sun: conceptualization, supervision, writing-reviewing and editing and funding acquisition.

Availability of data and material

The datasets supporting the conclusions of this article were available in the NCBI (PRJNA794722, https://www.ncbi.nlm.nih.gov/bioproject/PRJNA794722; PRJNA513244, https://www.ncbi.nlm.nih.gov/bioproject/PRJNA513244). The authors declare that all data supporting the results of this study were available within the article and Supplemental material. Further information and requests for resources and reagents should be directed to and will be fulfilled by the corresponding author.

Conflicts of interest

The authors declare no conflicts of interest.

Appendix A. Supporting information

Supporting data to this article can be found online at https://doi.org/10.1016/j.apsb.2023.08.002.

References

1. Beyer G, Habtezion A, Werner J, Lerch MM, Mayerle J. Chronic pancreatitis. *Lancet* 2020;**396**:499–512.
2. Kleeff J, Whitcomb DC, Shimosegawa T, Esposito I, Lerch MM, Gress T, et al. Chronic pancreatitis. *Nat Rev Dis Prim* 2017;**3**:17060.
3. Tamura K, Yu J, Hata T, Suenaga M, Shindo K, Abe T, et al. Mutations in the pancreatic secretory enzymes CPA1 and CPB1 are associated with pancreatic cancer. *Proc Natl Acad Sci U S A* 2018;**115**:4767–72.
4. Capurso G, Signoretti M, Archibugi L, Stigliano S, Fave GD. Systematic review and meta-analysis: small intestinal bacterial overgrowth in chronic pancreatitis. *United European Gastroenterol J* 2016;**4**:697–705.
5. Hm NC, Bashir Y, Dobson M, Ryan BM, Duggan SN, Conlon KC. The prevalence of small intestinal bacterial overgrowth in non-surgical patients with chronic pancreatitis and pancreatic exocrine insufficiency (PEI). *Pancreatology* 2018;**18**:379–85.
6. El Kurdi B, Babar S, El Iskandarani M, Bataineh A, Lerch MM, Young M, et al. Factors that affect prevalence of small intestinal

bacterial overgrowth in chronic pancreatitis: a systematic review, meta-analysis, and meta-regression. *Clin Transl Gastroenterol* 2019; **10**:e00072.
7. Pan LL, Li BB, Pan XH, Sun J. Gut microbiota in pancreatic diseases: possible new therapeutic strategies. *Acta Pharmacol Sin* 2021;**42**: 1027−39.
8. Han MM, Zhu XY, Peng YF, Lin H, Liu DC, Li L. The alterations of gut microbiota in mice with chronic pancreatitis. *Ann Transl Med* 2019;**7**:464.
9. Jandhyala SM, Madhulika A, Deepika G, Rao GV, Reddy DN, Subramanyam C, et al. Altered intestinal microbiota in patients with chronic pancreatitis: implications in diabetes and metabolic abnormalities. *Sci Rep* 2017;**7**:43640.
10. Sokol H, Pigneur B, Watterlot L, Lakhdari O, Bermúdez-Humarán LG, Gratadoux JJ, et al. *Faecalibacterium prausnitzii* is an anti-inflammatory commensal bacterium identified by gut microbiota analysis of Crohn disease patients. *Proc Natl Acad Sci U S A* 2008; **105**:16731−6.
11. Thomas LV, Ockhuizen T, Suzuki K. Exploring the influence of the gut microbiota and probiotics on health: a symposium report. *Br J Nutr* 2014;**112**(Suppl 1):S1−18.
12. Frost F, Weiss FU, Sendler M, Kacprowski T, Rühlemann M, Bang C, et al. The gut microbiome in patients with chronic pancreatitis is characterized by significant dysbiosis and overgrowth by opportunistic pathogens. *Clin Transl Gastroenterol* 2020;**11**:e00232.
13. Singh VK, Yadav D, Garg PK. Diagnosis and management of chronic pancreatitis: a review. *JAMA* 2019;**322**:2422−34.
14. Apte M, Pirola R, Wilson J. The fibrosis of chronic pancreatitis: new insights into the role of pancreatic stellate cells. *Antioxidants Redox Signal* 2011;**15**:2711−22.
15. Xue J, Sharma V, Hsieh MH, Chawla A, Murali R, Pandol SJ, et al. Alternatively activated macrophages promote pancreatic fibrosis in chronic pancreatitis. *Nat Commun* 2015;**6**:7158.
16. Sun J, Xu M, Ortsater H, Lundeberg E, Juntti-Berggren L, Chen YQ, et al. Cathelicidins positively regulate pancreatic beta-cell functions. *Faseb J* 2016;**30**:884−94.
17. Aggarwal H, Pathak P, Singh V, Kumar Y, Shankar M, Das B, et al. Vancomycin-induced modulation of Gram-positive gut bacteria and metabolites remediates insulin resistance in iNOS knockout mice. *Front Cell Infect Microbiol* 2022;**11**:795333.
18. Sasseville D. Neomycin. *Dermatitis* 2010;**21**:3−7.
19. Tian Y, Xu Q, Sun L, Ye Y, Ji G. Short-chain fatty acids administration is protective in colitis-associated colorectal cancer development. *J Nutr Biochem* 2018;**57**:103−9.
20. Tandon RK, Sato N, Garg PK, Group CS. Chronic pancreatitis: Asia−Pacific consensus report. *J Gastroenterol Hepatol* 2002;**17**: 508−18.
21. Ren Z, Pan LL, Huang Y, Chen H, Liu Y, Liu H, et al. Gut microbiota-CRAMP axis shapes intestinal barrier function and immune responses in dietary gluten-induced enteropathy. *EMBO Mol Med* 2021;**13**: e14059.
22. Wu C, Li M, Chen W. Characteristics of gut microbiota in cerulein-induced chronic pancreatitis. *Diabetes Metab Syndr Obes* 2021;**14**: 285−94.
23. Memba R, Duggan SN, Ni Chonchubhair HM, Griffin OM, Bashir Y, O'Connor DB, et al. The potential role of gut microbiota in pancreatic disease: a systematic review. *Pancreatology* 2017;**17**:867−74.
24. Akshintala VS, Talukdar R, Singh VK, Goggins M. The gut microbiome in pancreatic disease. *Clin Gastroenterol Hepatol* 2019;**17**:290−5.
25. Benjamin O, Lappin SL. *Chronic pancreatitis*. Treasure Island (FL): StatPearls; 2022.
26. Reding T, Bimmler D, Perren A, Sun LK, Fortunato F, Storni F, et al. A selective COX-2 inhibitor suppresses chronic pancreatitis in an animal model (WBN/Kob rats): significant reduction of macrophage infiltration and fibrosis. *Gut* 2006;**55**:1165−73.
27. Pan L, Yu H, Fu J, Hu J, Xu H, Zhang Z, et al. Berberine ameliorates chronic kidney disease through inhibiting the production of gut-derived uremic toxins in the gut microbiota. *Acta Pharm Sin B* 2023;**13**:1537−53.
28. Reichardt N, Duncan SH, Young P, Belenguer A, McWilliam Leitch C, Scott KP, et al. Phylogenetic distribution of three pathways for propionate production within the human gut microbiota. *ISME J* 2014;**8**:1323−35.
29. Zhang Z, He S, Cao X, Ye Y, Yang L, Wang J, et al. Potential prebiotic activities of soybean peptides Maillard reaction products on modulating gut microbiota to alleviate aging-related disorders in D-galactose-induced ICR mice. *J Funct Foods* 2020;**65**:103729.
30. Park BS, Lee JO. Recognition of lipopolysaccharide pattern by TLR4 complexes. *Exp Mol Med* 2013;**45**:e66.
31. Fan J, Duan L, Wu N, Xu X, Xin J, Jiang S, et al. Baicalin ameliorates pancreatic fibrosis by inhibiting the activation of pancreatic stellate cells in mice with chronic pancreatitis. *Front Pharmacol* 2020;**11**: 607133.
32. Tsuji Y, Watanabe T, Kudo M, Arai H, Strober W, Chiba T. Sensing of commensal organisms by the intracellular sensor NOD1 mediates experimental pancreatitis. *Immunity* 2012;**37**:326−38.
33. Talukdar R, Karvellas CJ, Talukdar R, Talukdar R, Talukdar R, Jandhyala SM, et al. Altered gut microbiota in patients with chronic pancreatitis is associated with gut barrier dysfunction and metabolic abnormalities. *Clin Gastroenterol Hepatol* 2017;**15**:153.
34. Sun J, Furio L, Mecheri R, van der Does Anne M, Lundeberg E, Saveanu L, et al. Pancreatic β-cells limit autoimmune diabetes *via* an immunoregulatory antimicrobial peptide expressed under the influence of the gut microbiota. *Immunity* 2015;**43**:304−17.
35. Lorchner H, Hou Y, Adrian-Segarra JM, Kulhei J, Detzer J, Gunther S, et al. Reg proteins direct accumulation of functionally distinct macrophage subsets after myocardial infarction. *Cardiovasc Res* 2018; **114**:1667−79.
36. Furusawa Y, Obata Y, Fukuda S, Endo TA, Nakato G, Takahashi D, et al. Commensal microbe-derived butyrate induces the differentiation of colonic regulatory T cells. *Nature* 2013;**504**:446−50.
37. Smith PM, Howitt MR, Panikov N, Michaud M, Gallini CA, Bohlooly YM, et al. The microbial metabolites, short-chain fatty acids, regulate colonic Treg cell homeostasis. *Science* 2013;**341**: 569−73.
38. Pan L, Han P, Ma S, Peng R, Wang C, Kong W, et al. Abnormal metabolism of gut microbiota reveals the possible molecular mechanism of nephropathy induced by hyperuricemia. *Acta Pharm Sin B* 2020;**10**:249−61.
39. Rooks MG, Garrett WS. Gut microbiota, metabolites and host immunity. *Nat Rev Immunol* 2016;**16**:341−52.
40. Huang G, Zhang S, Zhou C, Tang X, Li C, Wang C, et al. Influence of *Eimeria falciformis* infection on gut microbiota and metabolic pathways in mice. *Infect Immun* 2018;**86**. 000733-18.
41. Frost F, Kacprowski T, Ruhlemann M, Bulow R, Kuhn JP, Franke A, et al. Impaired exocrine pancreatic function associates with changes in intestinal microbiota composition and diversity. *Gastroenterology* 2019;**156**:1010−5.
42. Iljazovic A, Roy U, Galvez EJC, Lesker TR, Zhao B, Gronow A, et al. Perturbation of the gut microbiome by *Prevotella* spp. enhances host susceptibility to mucosal inflammation. *Mucosal Immunol* 2021;**14**: 113−24.
43. Hsiao EY, McBride SW, Hsien S, Sharon G, Hyde ER, McCue T, et al. Microbiota modulate behavioral and physiological abnormalities associated with neurodevelopmental disorders. *Cell* 2013;**155**: 1451−63.
44. Yoshida N, Emoto T, Yamashita T, Watanabe H, Hayashi T, Tabata T, et al. *Bacteroides vulgatus* and *Bacteroides dorei* reduce gut microbial lipopolysaccharide production and inhibit atherosclerosis. *Circulation* 2018;**138**:2486−98.
45. Marietta EV, Murray JA, Luckey DH, Jeraldo PR, Lamba A, Patel R, et al. Suppression of inflammatory arthritis by human gut-derived *Prevotella histicola* in humanized mice. *Arthritis Rheumatol* 2016; **68**:2878−88.

46. Scher JU, Sczesnak A, Longman RS, Segata N, Ubeda C, Bielski C, et al. Expansion of intestinal *Prevotella copri* correlates with enhanced susceptibility to arthritis. *Elife* 2013;**2**:e01202.
47. Ahuja M, Schwartz DM, Tandon M, Son A, Zeng M, Swaim W, et al. Orai1-mediated antimicrobial secretion from pancreatic acini shapes the gut microbiome and regulates gut innate immunity. *Cell Metabol* 2017;**25**:635−46.
48. Fusco A, Savio V, Donniacuo M, Perfetto B, Donnarumma G. Antimicrobial peptides human beta-defensin-2 and -3 protect the gut during *Candida albicans* infections enhancing the intestinal barrier integrity: *in vitro* study. *Front Cell Infect Microbiol* 2021; **11**:666900.
49. Li L, Bachem MG, Zhou S, Sun Z, Chen J, Siech M, et al. Pancreatitis-associated protein inhibits human pancreatic stellate cell MMP-1 and -2, TIMP-1 and -2 secretion and RECK expression. *Pancreatology* 2009;**9**:99−110.
50. Maslowski KM, Vieira AT, Ng A, Kranich J, Sierro F, Yu D, et al. Regulation of inflammatory responses by gut microbiota and chemoattractant receptor GPR43. *Nature* 2009;**461**:1282−6.
51. Song M, Wang J, Sun Y, Pang J, Li X, Liu Y, et al. Inhibition of gasdermin D-dependent pyroptosis attenuates the progression of silica-induced pulmonary inflammation and fibrosis. *Acta Pharm Sin B* 2022;**12**:1213−24.
52. Priyadarshini M, Wicksteed B, Schiltz GE, Gilchrist A, Layden BT. SCFA receptors in pancreatic beta cells: novel diabetes targets?. *Trends Endocrinol Metabol* 2016;**27**:653−64.
53. Zhu Y, Ouyang Z, Du H, Wang M, Wang J, Sun H, et al. New opportunities and challenges of natural products research: when target identification meets single-cell multiomics. *Acta Pharm Sin B* 2022; **12**:4011−39.
54. Li S, You J, Wang Z, Liu Y, Wang B, Du M, et al. Curcumin alleviates high-fat diet-induced hepatic steatosis and obesity in association with modulation of gut microbiota in mice. *Food Res Int* 2021;**143**:110270.
55. Nakanishi Y, Sato T, Ohteki T. Commensal Gram-positive bacteria initiates colitis by inducing monocyte/macrophage mobilization. *Mucosal Immunol* 2015;**8**:152−60.
56. Zigmond RE, Echevarria FD. Macrophage biology in the peripheral nervous system after injury. *Prog Neurobiol* 2019;**173**:102−21.